MIT
SEA
GRANT
PROGRAM

NOTCH GEOMETRY AND LAMINATE CONSTRUCTION EFFECTS ON THE FRACTURE TOUGHNESS OF LAMINATES FOR HULL CONSTRUCTION

by

William O. Bishop

John F. Mandell

Frederick J. McGarry

Massachusetts Institute of Technology

Cambridge, Massachusetts 02139

Report No. MITSG 73-15

November 30, 1973

NOTCH GEOMETRY AND LAMINATE CONSTRUCTION EFFECTS ON THE FRACTURE TOUGHNESS OF LAMINATES FOR HULL CONSTRUCTION

by

William O. Bishop
John F. Mandell
Frederick J. McGarry

Report No. MITSG 73-15
Index No. 73-315-Cfo

Abstract

The effects of notch geometry and ply stacking arrangement were investigated for fiberglass laminates of chopped fiber mat and woven roving reinforced polyester. The failure stress was found to be insensitive to notch root radius up to a value of approximately 0.10 inches. The crack flank angle was found to have little effect on the failure stress over a broad range. The results indicate that the validity of classical fracture mechanics is doubtful for this type of composites, and that a stress concentration approach may provide a more meaningful fracture criterion. The woven roving plies are shown to control the toughness of the laminate, while both roving and mat plies are significant in determining the tensile strength.

Table of Contents

	Page
Title Page	i
Abstract	ii
Table of Contents	iii
Introduction	1
Materials and Test Procedures	3
Results and Discussion	4
Conclusions	7
Acknowledgments	7
References	8
Tables I - III	9-13
Figures 1 - 8	14-21

Introduction

The effects of notch geometry on the failure strength of isotropic materials have been given considerable attention in the literature, particularly since the solution for an elliptical hole in an infinite plate under uniform applied tensile stress, σ, normal to the major axis of the ellipse was given by Inglis [1] as

$$\sigma_{max} = \sigma(1+2\sqrt{c/p}) \tag{1}$$

where σ_{max} is the maximum stress at the notch tip, c is the half-length of the ellipse, and p is the root-radius. The important dimensions of a notch of arbitrary shape are generally accepted to be its overall length normal to the maximum applied stress and the radius at the root [2].

For the case of a crack with a vanishingly small root radius, the distribution of stress parallel to the load, σ_{yy}, near the crack tip is given by [3]

$$\sigma_{yy} = \frac{\sigma\sqrt{\pi c}}{\sqrt{2\pi r}}\left[\frac{3}{4}\cos(\theta/2) + \frac{1}{4}\cos(5\theta/2)\right] \tag{2}$$

where r is the distance from the crack tip and θ is the angle from the crack axis. Equations (1) and (2) may be modified for anisotropic elastic constants without any change in the basic form of either [4].

Both of the above relationships assume elastic behavior of the material. Fracture criteria based on the maximum stress, σ_{max}, or stress intensity factor, $K = \sigma\sqrt{\pi c}$, are generally valid only if regions of inelastic behavior

near the crack tip are much smaller than the characteristic specimen dimensions such as the crack length [4]. The observed behavior of high strength metals with a plastic zone size, r_y , much smaller than the crack length is illustrated by the following example: consider a series of experiments where cracks of various root radius, ρ, are machined into specimens which are loaded in tension. As shown in Figure 1, the applied stress at fracture, σ_f , will be insensitive to root radius below some critical value, ρ_o, and will increase with $\sqrt{\rho}$ for radii above ρ_o, as predicted by Equation (1) [5]. The value of ρ_o is generally of the order $r_y/10$, and represents the equivalent notch root radius produced by the plastic strain within the yielded zone [6]. The approximate domain of applicability of the sharp crack theory represented by Equation (2) is for notch radii less than ρ_o, while Equation (1) apparently applies to larger radii, with the additional restriction in both cases that the value of ρ_o be much less than the dominant specimen dimensions.

An alternative, but equivalent, criterion for fracture is the critical strain energy release rate, or fracture surface work, originally suggested by Griffith [7]. This criterion is a simple statement of the thermodynamic conditions necessary for crack extension, and, although often expressed as a function of the critical stress intensity factor, is not subject to the same stringent

restrictions on crack radius and plastic zone size as in the stress intensity factor [4]. The relatively large inherent crack tip radius which results from subcracking parallel to the fibers at the crack tip [8] may severely limit the applicability of the classical stress intensity factor for composite materials, but the modification to the strain energy release rate may be relatively insignificant [4].

Materials and Test Procedures

All laminates tested were a combination of Laminac 4155 polyester (American Cyanamid Co.) reinforced by E-glass fibers in the form of 1-1/2 oz/ft^2 chopped fiber mat and 18 oz/yd^2 Style 61 woven roving (Uniglass Industries); the woven roving was oriented with the warp direction perpendicular to the load. Laminates were fabricated by the hand layup method and cured at room temperature.

Test specimens for notch geometry studies were cut roughly to size by a diamond-edged wheel and then machined to final dimensions by a TensilKut router. Desired radii were obtained by drilling with carbide drills, and notch flanks were cut with a 0.018 inch thick diamond-edged wheel. Ultimate strength specimens were machined on a TensilKut router to the shape shown in Figure 2, which was found to give the highest percentage of failures in

the gage section, approximately 50 percent, of the shapes investigated. Cleavage test specimens were machined in the same fashion as other notched specimens, and aluminum strips were then bonded to the sides with epoxy adhesive as shown in Figure 3, to give sufficient stiffness to avoid buckling of the specimen prior to fracture.

All specimens were tested in an Instron universal testing machine under laboratory temperature and humidity conditions and at a displacement rate of 0.05 inches per minute. The load-deflection curve for notched and unnotched tension specimens was approximately linear to fracture, and the strength was determined from the maximum load attained. The critical strain energy release rate was determined from the load-deflection curve as indicated in Figure 4 by measuring the area under a cycle of loading-crack extension and unloading with a planimeter; this procedure has been used previously and is discussed elsewhere [8].

Results and Discussion

The effect of notch root radius on the applied stress at fracture is given in Figure 5 for a laminate of MRMRM construction, where M represents a mat ply and R represents a woven roving ply. Although the shape of the curve is similar to that in Figure 1 for metals, the radius below which the fracture stress is relatively

constant is approximately 0.10 inches, one to three orders of magnitude greater than that observed for high strength metals [59]. Table 1 gives additional data including the stress on the net cross-section between notches at failure and the critical stress intensity factor, K_Q, calculated from the isotropic solution for a finite width specimen with a sharp notch [10]. The average ultimate tensile strength, σUTS, and fiber volume fraction, V_f, for the laminates used in this portion of the study were 23.8 ksi and 0.336 respectively; Table 1 indicates that the net section stress at fracture for the sharper notches was approximately half of the ultimate strength, while for larger radii the value reached a maximum of over 90 percent of the ultimate strength. The calculated value of K_Q was insensitive to notch radius for radii up to approximately 0.10 inches, and then increased for larger radii. A typical specimen of this type is shown after fracture in Figure 6.

The notch radius data indicate that the value of ρ_o for this material is approximately o.10 inches. Since this value is of the same order of magnitude as the length of typical cracks to be anticipated in applications, the validity of the classical stress intensity factor calculation is doubtful, and the use of a stress concentration factor criterion may be more meaningful. It is apparent that, while crack propagagation occurs in the absence of

any general yielding of the material, the crack tip is inherently orders of magnitude less sharp than is generally anticipated for materials which fail in a brittle fashion.

Figure 7 and Table 2 give the results of similar tests where the notch radius was held constant and the flank angle was varied. The flank angle is found to have little effect on the applied stress at fracture except for very large flank angles, which, in the limit, approach the unnotched case.

Table 3 gives the results of varying the ply stacking sequence of the laminate, where, as before, M represents a mat ply and R represents a woven roving ply; N_R represents the number of woven roving plies in a laminate. The data indicate that the woven roving plies dominate the value of critical strain energy release rate, G_Q, but that the ultimate strength depends upon both components. Since the applied stress at fracture for a notched sample varies with the square root of G_Q [4], the load carrying ability of a flawed member clearly depends almost entirely on the roving plies. It should be noted that the cleavage samples with bonded aluminum strips may not give a reliable measure of G_Q due to interference of the aluminum strips with the extension of the subcracking zone at the crack tip. However, the results are expected to give an accurate comparison of the relative toughness of the various ply stacking arrangements. Figure 8 shows

a typical cleavage specimen after crack propagation.

Conclusions

The results indicate that the strength of a notched member is insensitive to the notch root radius up to a value of approximately 0.10 inches, and is relatively insensitive to crack flank angle over a broad range. The applicability of the classical stress intensity factor is doubtful due to the inherent bluntness of a propagating crack, and a stress concentration factor approach may provide a more meaningful criterion. Variations in the ply stacking arrangement indicate that the woven roving plies are primarily responsible for the toughness, while both woven roving and chopped fiber mat plies contribute significantly to the ultimate strength.

Acknowledgments

The general research program on the fracture behavior of fibrous reinforced composites, from which this report derives, receives support from The Dow Chemical Company, the Air Force Materials Laboratory (USAF Contract F33615-72-C-1686), the NOAA Office of Sea Grant, Grant No. NG43-72, and the M.I.T. Center of Materials Science and Engineering (NSF Contract GH-33653). This support is gratefully acknowledged by the authors.

References

1. C. E. Inglis, Trans. Naval Arch., Vol. 55. No. 1, p. 219.

2. A. Kelly, Strong Solids, Clarendon, Oxford (1966).

3. G. R. Irwin, "Analysis of Stresses and Strains Near the Tip of a Crack Traversing a Plate," Trans. ASME, J. App. Mech. (1957), p. 361.

4. G. C. Sih and H. Liebowitz, in Fracture, Vol. 2, edited by H. Liebowitz, Academic Press (1968).

5. J. H. Malherin, D. F. Armiento, and H. Marcess, "Fracture Characteristics of High Strength Aluminum Alloys Using Specimens with Variable Notch-Root Radii," Paper presented to Am. Soc. Mech. Engr. meeting, Philadelphia (1963).

6. H. Neuber, "Kerbspannungslehre," Berlin, Julius Springer (1937).

7. A. A. Griffith, "The Phenomena of Rupture and Flow in Solids," Phil. Trans. Roy. Soc. (London), A221 (1970), p. 163.

8. F. J. McGarry and J. F. Mandell, "Fracture Toughness of Fibrous Glass Reinforced Plastic Composites," Proc. 27th Reinforced Plastics/Composites Div., SPI (1972), Section 9A.

9. "Fracture Testing of High-Strength Sheet Materials," Materials Research Standards, Vol. 1, (1966), p. 716.

10. D. L. Bowie, "Rectangular Tensile Sheet with Symmetric Edge Cracks," Paper 64-APM-3, ASME (1964).

Table 1

Effect of Notch Root Radius for Ply Configuration

(M/R/M/R/M)*

Notch Radius (in)	σ_f (Applied Stress at Fracture ksi)	σ_{net} (Average Stress on Net Cross-Section at Fracture, ksi)	$\frac{\sigma_{net}}{\sigma UTS}$	K_Q (Fracture Toughness, ksi$\sqrt{in}$)
0.01	6.7	13.4	.56	13.4
0.01	6.6	13.2	.55	13.2
0.01	6.5	13.0	.54	13.0
0.03	6.5	13.0	.54	13.0
0.03	5.5	10.9	.46	11.0
0.03	6.6	13.1	.55	13.2
0.06	6.1	12.2	.51	12.2
0.06	6.5	12.9	.54	12.9
0.06	5.7	11.4	.48	11.5
0.125	6.5	13.0	.54	13.0
0.125	5.7	11.4	.47	11.4
0.125	6.9	13.7	.57	13.7
0.25	8.5	16.9	.71	16.9
0.25	7.7	15.4	.64	15.5
0.25	5.7	11.4	.48	11.4

Table 1
(continued)

0.50	8.2	16.3	.69	16.7
0.50	5.9	11.8	.49	11.8
0.50	6.5	13.0	.54	13.0
1.00	8.8	17.5	.73	17.5
1.00	8.4	16.7	.69	16.7
1.00	10.7	21.13	.89	21.4
2.00	11.0	21.9	.92	22.0
2.00	8.7	17.3	.72	17.3
2.00	9.2	18.3	.77	18.3

---

* σ_f = LOAD/ (w x t)

σ_{net} = LOAD/[t x (w-2c)]

$K_Q = \sigma_f Y \sqrt{c}$, where Y = 2.0 [11].

where: w is the specimen width

c is the notch depth

t is the thickness

Table 2

Effect of Notch Flank Length

for Ply Configuration M/R/M/R/M

Flank Dimension, l (in)	σ_f (Applied Stress at Fracture, ksi)	σ_{net} (Average Stress on Net Cross-section at Fracture, ksi)	$\frac{\sigma_{net}}{\sigma_{UTS}}$	K_Q (Fracture Toughness, ksi $\sqrt{in}$)
0.13	6.5	13.0	.54	13.0
0.13	5.5	11.0	.46	11.0
0.13	6.6	13.1	.55	13.1
0.50	5.5	11.0	.46	11.0
0,50	6,0	11.9	.49	11.9
0.50	6.5	12.9	.54	12.9
1.00	5.4	10.8	.45	10.8
1.00	6.0	11.9	.44	11.9
1.00	5.9	11.8	.49	11.8
2.50	6.4	12.8	.53	12.8
2.50	6.5	12.9	.54	12.9
2.50	5.9	11.7	.49	11.8
5.00	8.0	16.0	.67	16.1
5.00	7.4	14.8	.62	14.9
5.00	8.1	16.2	.68	16.3

Table 2
(continued)

10.00	8.1	16.2	.68	16.3
10.00	9.5	18.9	.79	18.9
10.00	7.3	14.6	.61	14.7

Table 3

Toughness and Strength

for Various Ply Stacking Arrangements*

Ply Arrangement	Fiber Volume Fraction, V_f	ULTIMATE TENSILE STRENGTH UTS (ksi)	ULTIMATE TENSILE STRENGTH $\sigma_{UTS}(\frac{0.40}{V_f})$ (ksi)	CRITICAL STRAIN ENERGY RELEASE RATE G_Q (in-lb/in^2)	CRITICAL STRAIN ENERGY RELEASE RATE $(G_Q)_R$ (in-lb/in-R ply)
RRRR	0.50	31.7	25.4	325	6.90
RMRMRMR	0.39	30.2	31.0	259	7.96
RRMMMRR	0.42	24.5	23.2	231	7.28
MRRMRRM	0.39	27.7	28.4	194	6.43
MRMRMRMRM	0.38	26.3	27.7	186	8.83

* $(G_Q)_R = G_Q\ (\frac{t}{n_R})$ (fracture work per woven roving ply

where n is the total number of plies and n_R is the number of woven roving plies)

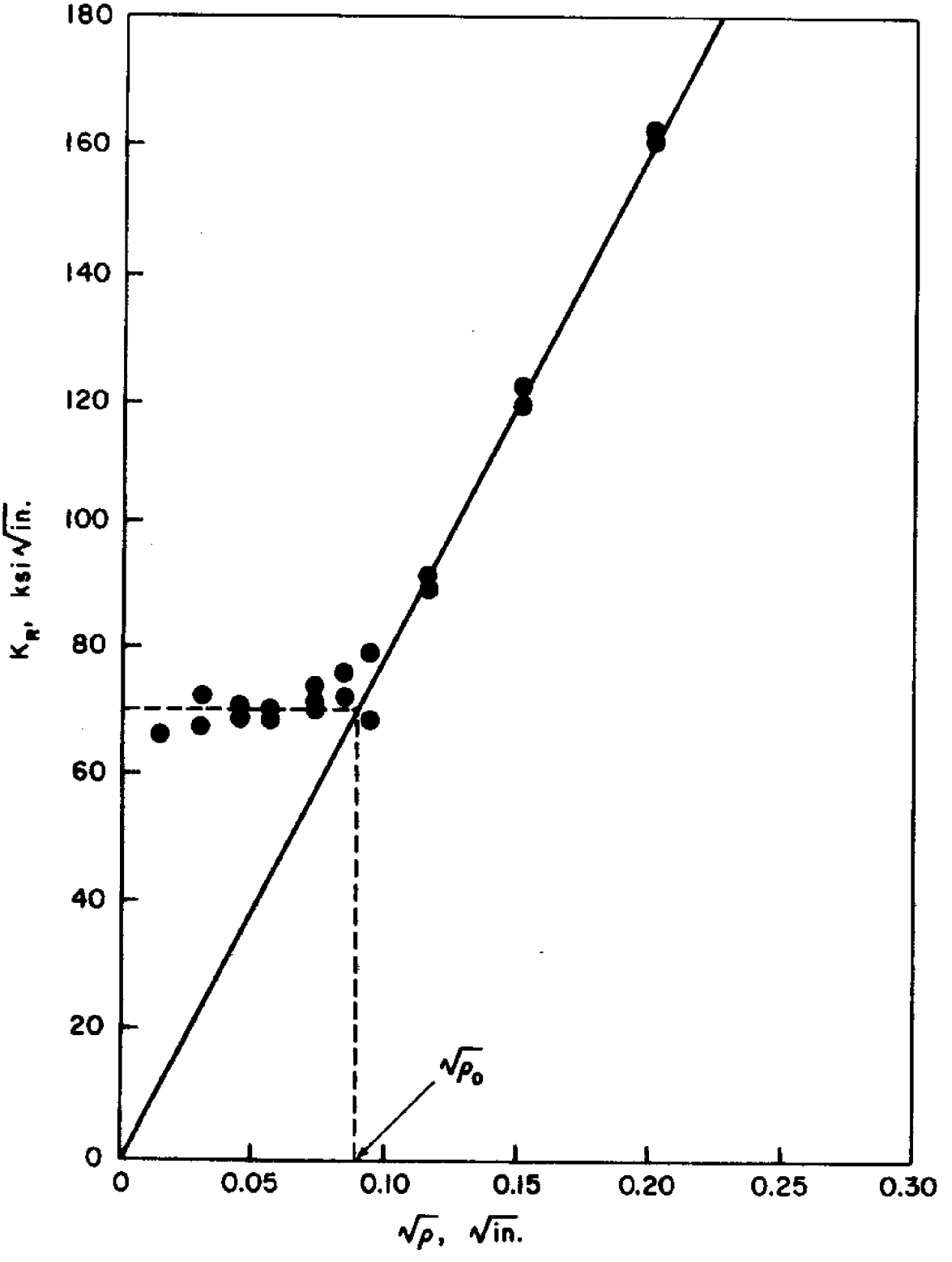

FIGURE 1.

INFLUENCE OF NOTCH SHARPNESS ON THE APPARENT CRITICAL VALUE OF K_R, A MODIFIED VERSION OF THE STRESS INTENSITY FACTOR, FOR 7075-T6 ALUMINUM. (FROM REFERENCE [5].)

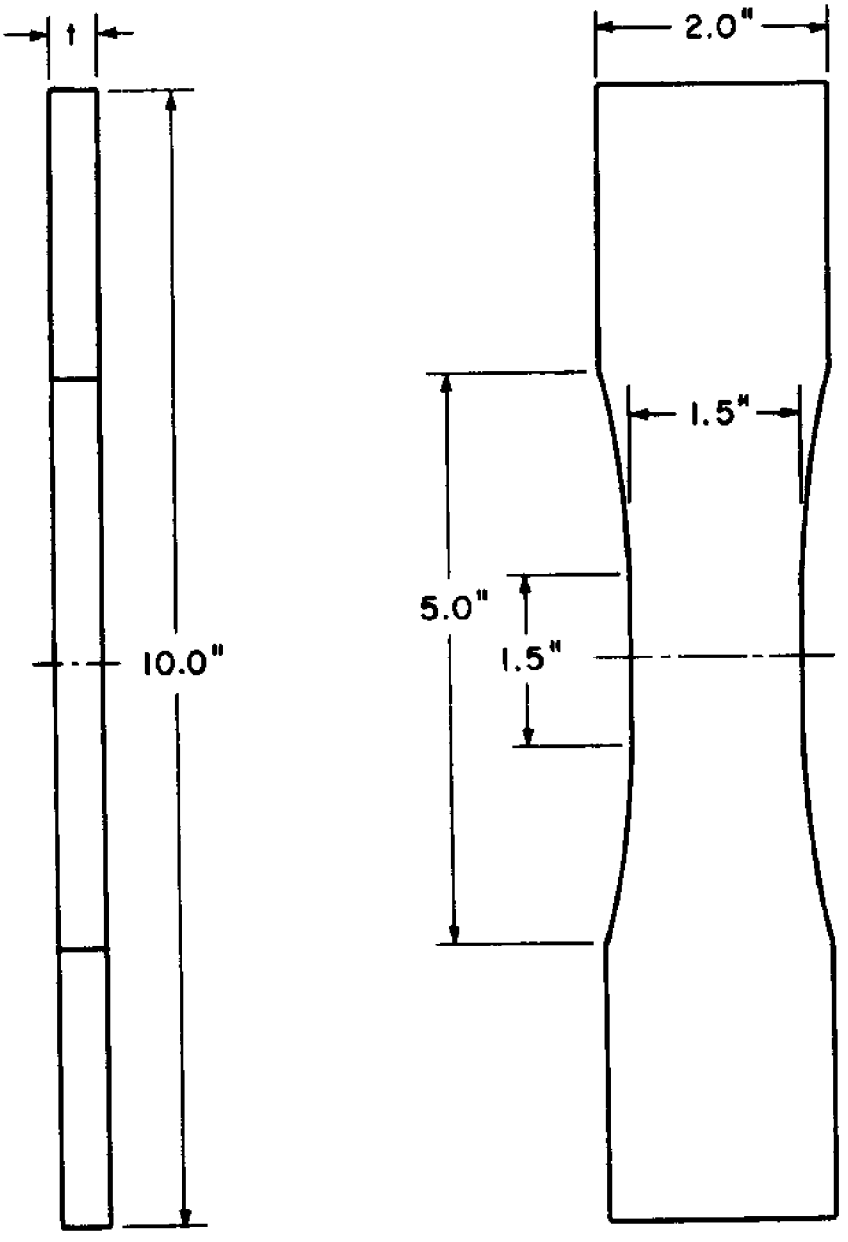

FIGURE 2.

ULTIMATE TENSILE STRENGTH SPECIMEN.

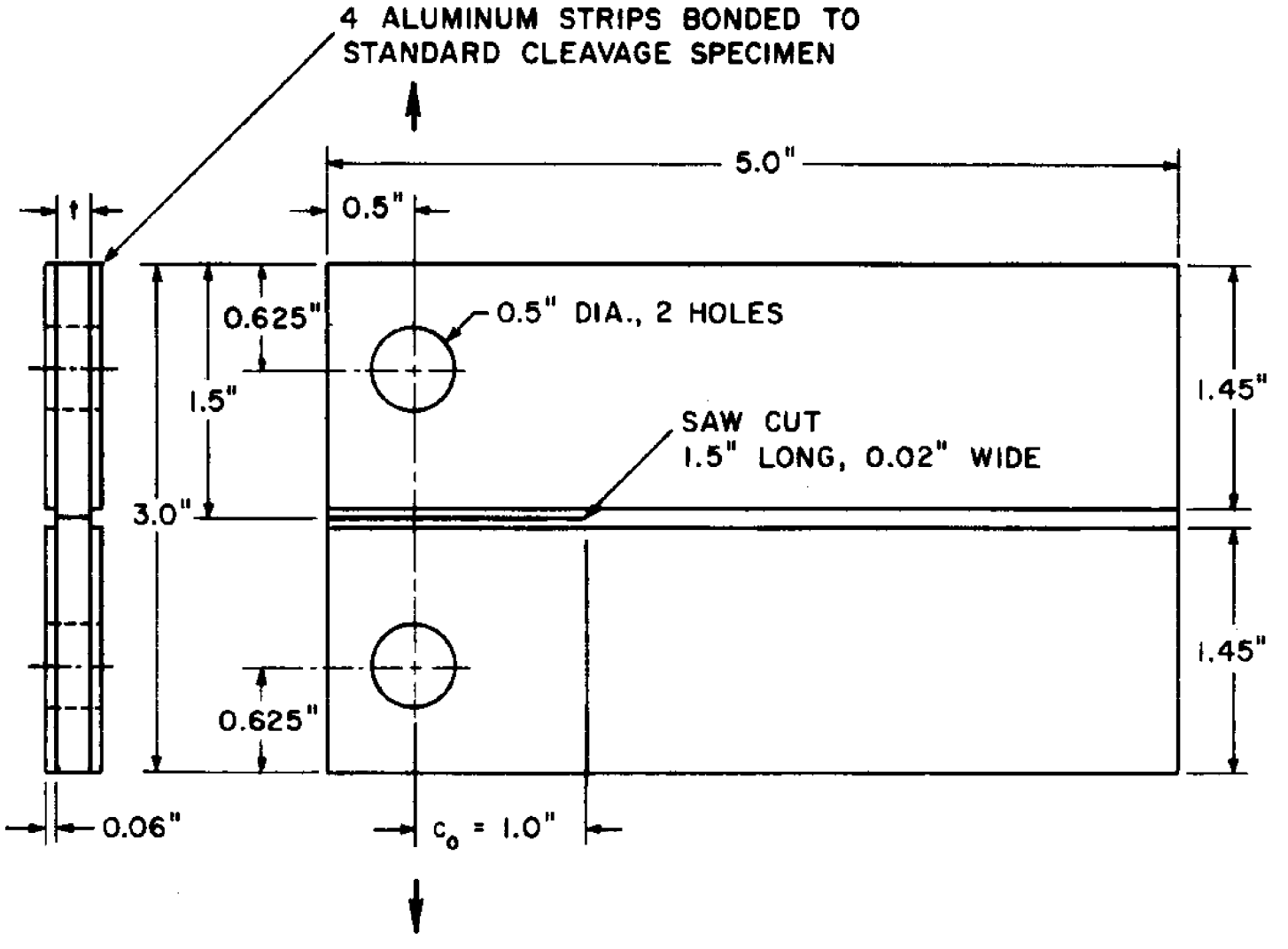

FIGURE 3.

MODIFIED CLEAVAGE SPECIMEN.

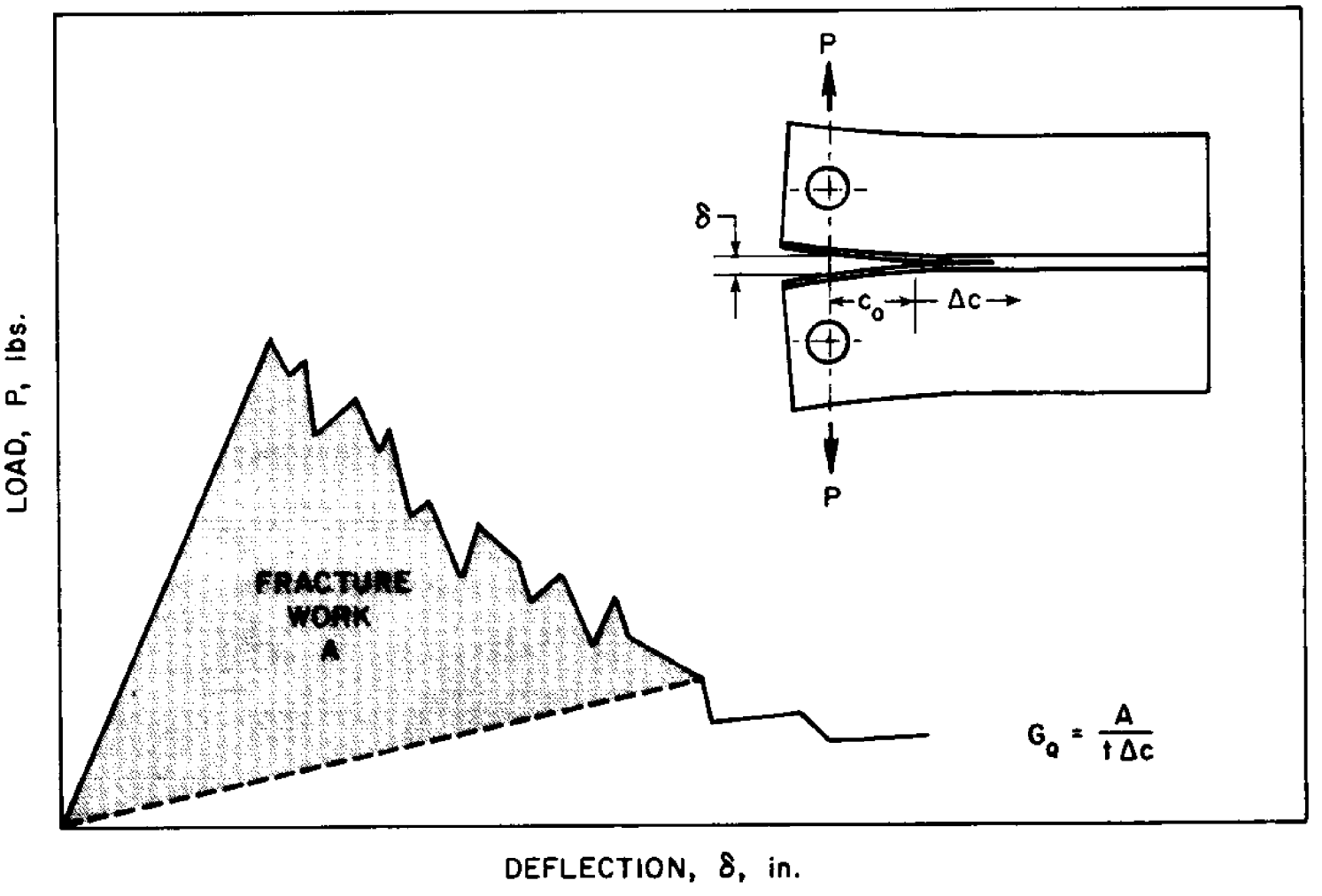

FIGURE 4.

TYPICAL LOAD-DEFLECTION CURVE FOR CLEAVAGE TESTS.

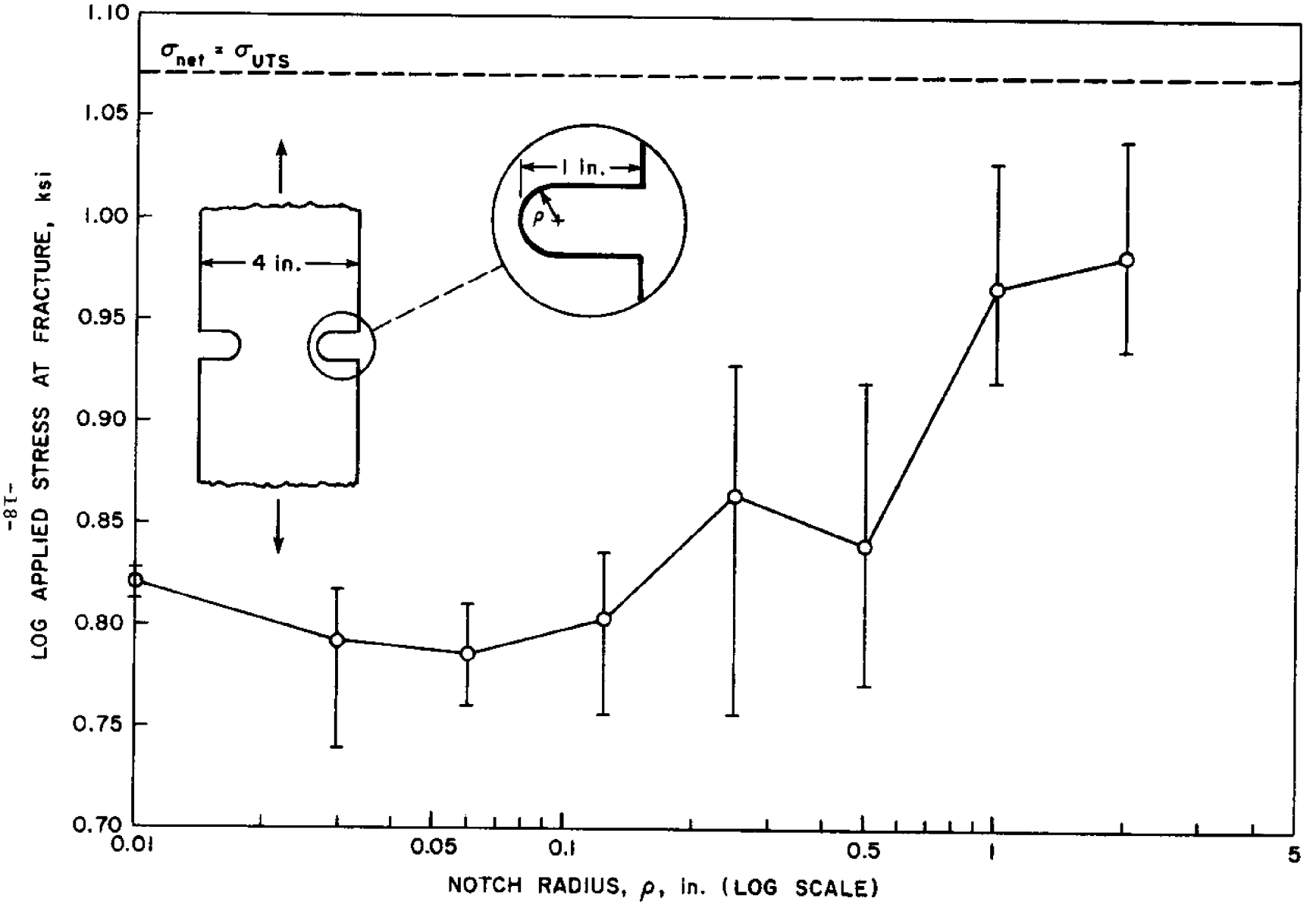

FIGURE 5.

EFFECT OF NOTCH RADIUS ON FRACTURE STRESS FOR 5 PLY, 0° ROVING/MAT/POLYESTER.

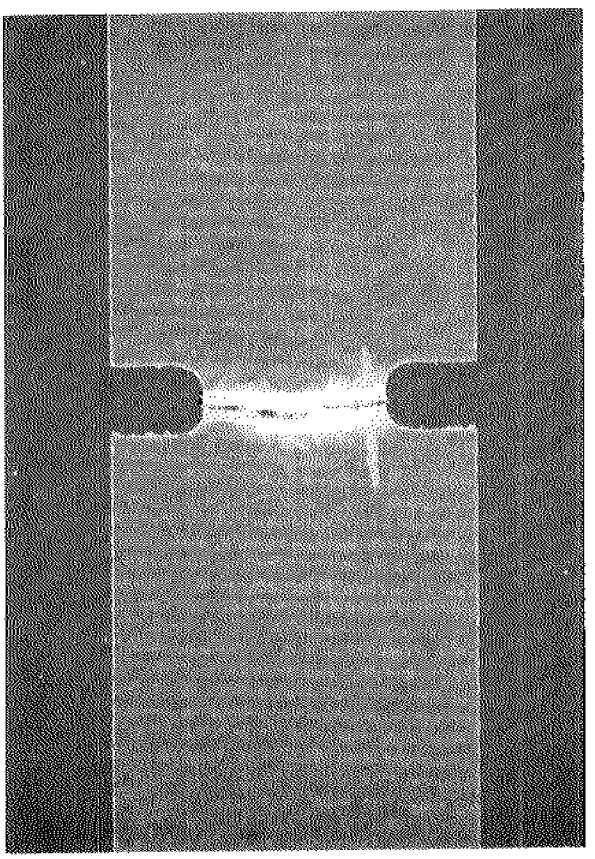

FIGURE 6.

FRACTURED SPECIMEN WITH
0.5 INCH NOTCH ROOT RADIUS.

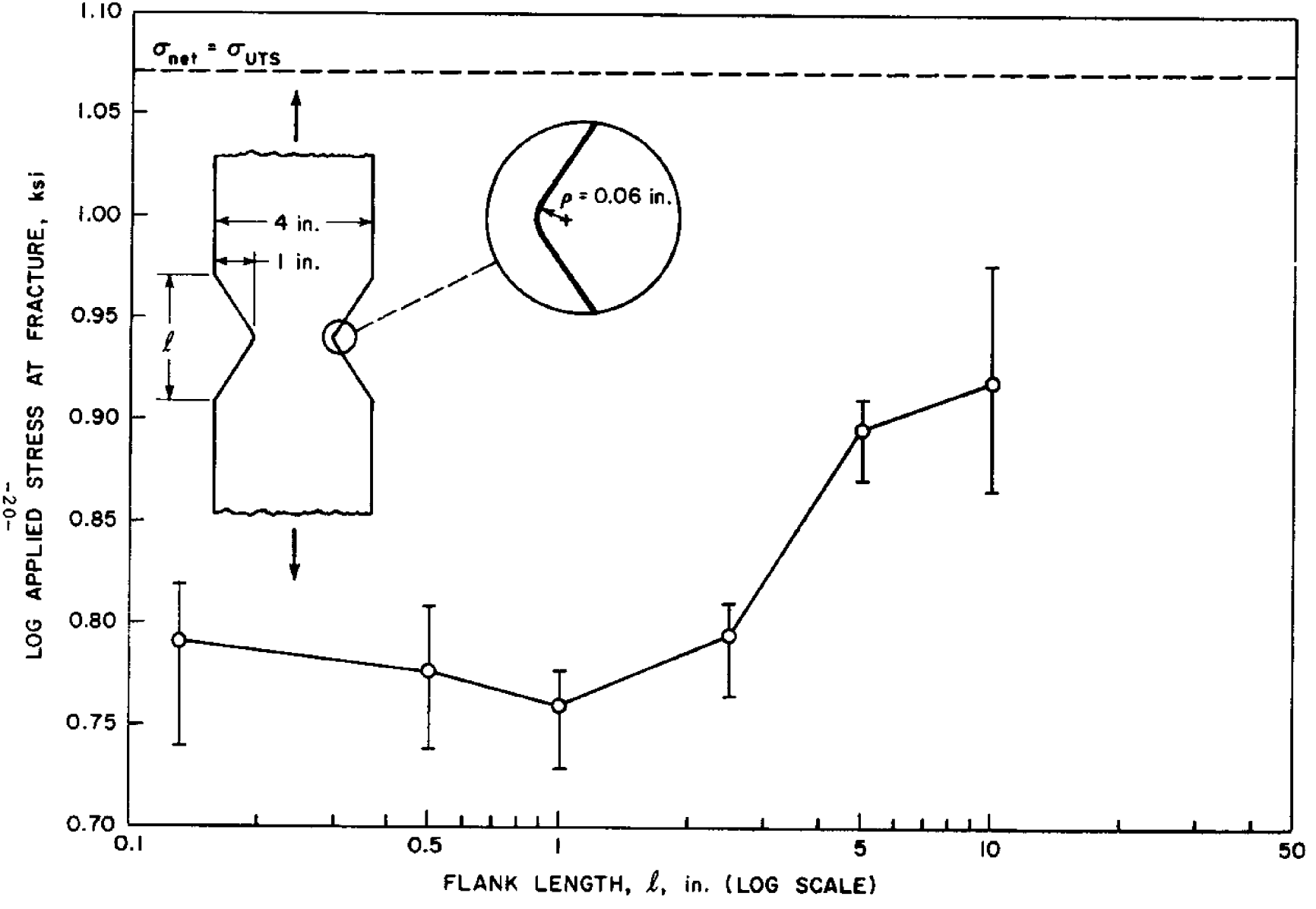

FIGURE 7.

EFFECT OF NOTCH FLANK LENGTH ON FRACTURE STRESS FOR 5 PLY, 0° ROVING/MAT/POLYESTER.

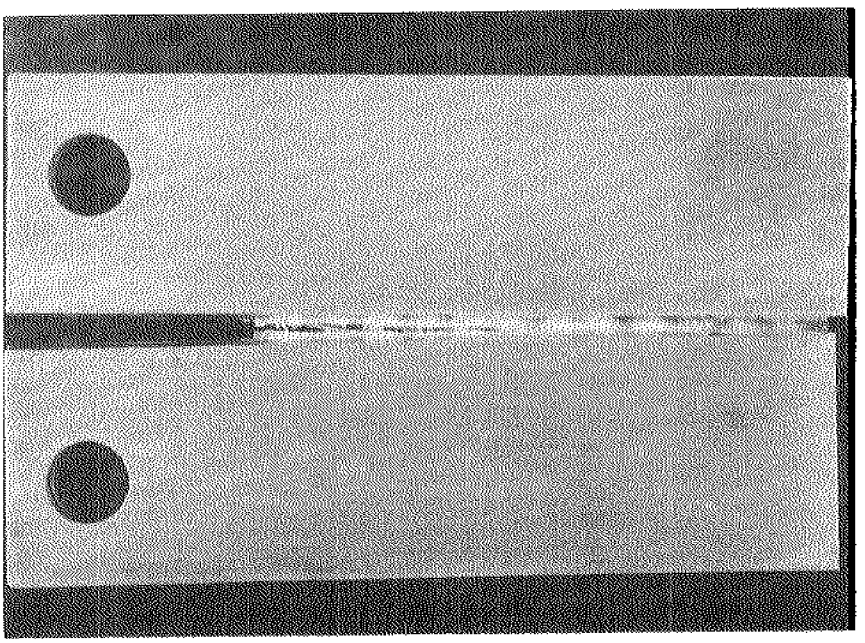

FIGURE 8.

CLEAVAGE SPECIMEN AFTER
CRACK PROPAGATION.